Available online at www.sciencedirect.com

ScienceDirect

Physics Procedia 3 (2010) 651–658

Physics Procedia

www.elsevier.com/locate/procedia

International Congress on Ultrasonics, Universidad de Santiago de Chile, January 2009

# Theory and experiment for single lens fiber optical microphone

João Marcos Salvi Sakamoto *, Gefeson Mendes Pacheco

*Instituto Tecnológico de Aeronáutica, Praça Marechal Eduardo Gomes, 50 – Vila das Acácias, CEP 12228-900, São José dos Campos, SP, Brasil*

**Abstract**

This work reports a theory for the single lens fiber optical microphone. Computational simulation and experimental results were compared presenting good agreement. It is shown that the operating principle of this microphone is based in membrane tilt angle variation rather than membrane longitudinal displacement.

*Keywords:* fiber optical microphone; acoustic sensor; nondestructive essay

## 1. Introduction

Interest on fiber optical microphone, FOM, is related to the advantages that an optical sensor has over conventional sensors, such as electrical and chemical passiveness and electromagnetic interference immunity. In addition, long distances between the microphone and the electronic circuit are supported due to the low loss characteristic of optical fiber. These features make feasible the employ of a FOM as an alternative way to applications in surveillance, military, medicine, robotics, and noncontact or nondestructive essays [1]-[4].

In the FOM configuration proposed in this work, differently from classic configurations [5], [6] a lens is used and the principle of operation based in back and forward movement of membrane is not valid anymore. Feldmann and Büttgenbach [7] developed a two lens fiber optical microphone and used the classical approach to explain the behavior of this microphone, but unlike suggested by these authors, a back and forward movement will not cause the light modulation since lens focus the parallels beams at the same point.

The theoretical analysis presented in an early work by the authors [8], provided the computational simulation and in this work it is compared to experimental data.

* Corresponding author. Tel.:+55-012-39476819; fax:+55-012-39478878.
*E-mail address*: jmss@ita.br

doi:10.1016/j.phpro.2010.01.082

## 2. Theory

### 2.1. Microphone scheme

The proposed fiber optical microphone consists of two optical fibers (transmitting and receiving ones), one positive lens, and one reflective membrane, as shown in Fig. 1. The light emerges from the transmitting fiber in a conical shape limited by the critical angle $\theta_o$, until it reaches the lens. The distance, $d_o$, between the lens and the transmitting fiber is set to obtain a collimated beam after lens. Supposing that membrane is tilted by an angle $\theta$ relative to $y$ axis, the collimated beam reaches the membrane with incidence angle $\theta$ relative to the membrane normal, and is reflected with the same angle. Total deviation is equal to $2\theta$. After going through the lens again, the beam is focused reaching the receiving fiber core. The tilt of the membrane is necessary to light impinge the core of receiving fiber since transmitting and receiving fibers are spatially separated.

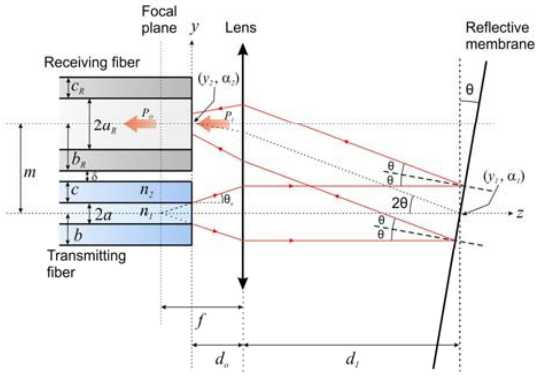


Fig.1 Detailed scheme of fiber optical microphone head with a single lens and tilted membrane.

The parameters shown in Fig. 1 are the following: $a$, $b$ and $c$ are core radius, cladding radius, and cladding thickness of transmitting fiber; $n_1$ and $n_2$ are the refractive indexes of core and cladding, respectively; $a_r$, $b_r$ and $c_r$ are core radius, cladding radius and cladding thickness of receiving fiber; $m$ is the distance between the center of fibers and $\delta$ is the gap between fibers; $d_1$ is the distance between lens and reflective membrane; $P_1$ is the total power of the beam incident in the entrance plane of receiving fiber, $z = 0$, and $P_o$ is the power coupled to receiving fiber core; $y_1$ and $\alpha_1$ are the height and angle of the center ray at membrane, or plane $z = d_o + d_1$; $y_2$ and $\alpha_2$ are the height and angle of the center ray at fibers plane, or $z = 0$. The angle $\theta_o$ is given by

$$\theta_o = \sin^{-1}\left(NA/n\right) \tag{1}$$

where $n$ is the air refractive index and $NA$ is the transmitting fiber numerical aperture, given by

$$NA = \sqrt{n_1^2 - n_2^2} \tag{2}$$

The distance $d_o$ is given by

$$d_o = f - a/\tan\left(\theta_o\right) \tag{3}$$

where $f$ is the lens focal distance.

In the next section power transfer coefficient, η, i.e., the ratio between the power coupled to the receiving fiber, $P_o$, and the total power incident on its surface, $P_I$, is calculated to determine how amplitude modulation of light occurs in this microphone.

### 2.2. Principle of operation

#### 2.2.1. Power transfer coefficient

The intensity distribution profile of the optical beam from transmitting fiber can be regarded as gaussian and can be written in cylindrical coordinate as

$$I(r) = I_I e^{\frac{-\Lambda r^2}{w^2}} \tag{4}$$

where $r$ is the radial coordinate, $I_I$ is the optical intensity at the center of the cross section plane, $\Lambda$ is a constant related to the modal power distribution in the fiber, and $w$ is the beam (or spot) radius. Integrating (4) over the total spot area, $S$, one can find the relation between the optical power $P_I$ and the optical intensity $I_I$ on the entrance plane of receiving fiber, as follows:

$$P_I = \iint I(r)dS = \int_0^{2\pi} d\phi \int_0^{\infty} I(r) r dr = \frac{\pi w^2}{\Lambda} I_I \tag{5}$$

where $dS$ is the area differential element of $S$. Then the optical intensity distribution in terms of $P_I$ can be written as

$$I(r) = \frac{\Lambda}{\pi w^2} P_I e^{\frac{-\Lambda r^2}{w^2}} \tag{6}$$

The optical power coupled to the receiving fiber can be calculated integrating (6) over incident light area on core:

$$P_o = \iint I(r)dS_R = P_I \frac{2\Lambda}{\pi w^2} \int_{r_1}^{r_2} \phi(r) r e^{\frac{-\Lambda r^2}{w^2}} dr \tag{7}$$

where $dS_R$ is the area differential element of the intersection area, $S_R$, between spot and fiber core. The angle between $y$ axis and the line connecting the center of spot to the intersection point of core and spot is given by

$$\phi(r) = \cos^{-1}\left(\frac{r^2 + d^2 - a_r^2}{2rd}\right) \tag{8}$$

Finally, regarding transmission losses in interface air-receiving fiber as a constant $\Gamma$, the power transfer coefficient is as follows:

$$\eta = \frac{P_o}{P_I} = \Gamma \frac{2\Lambda}{\pi w^2} \int_{r_1}^{r_2} \phi(r) r e^{\frac{-\Lambda r^2}{w^2}} dr \tag{9}$$

With (9) it is possible to calculate $\eta$ for each spot position relative to the center of receiving fiber. Such position determines the integration limits. The two parameters which the authors take in account as the cause of variations in spot positions are $d_I$ and $\theta$.

In Fig. 2, the $x$ and $y$ axis have the origin in center of transmitting fiber core. The $x'$ and $y'$ axis are placed in the center of spot and move with it. The parameter $d$ is the distance between center of receiving fiber core and center of spot, and is given by

$$d = m - y_2 \tag{10}$$

where the distance $m$ is

$$m = a + a_R + c + c_R + \delta \tag{11}$$

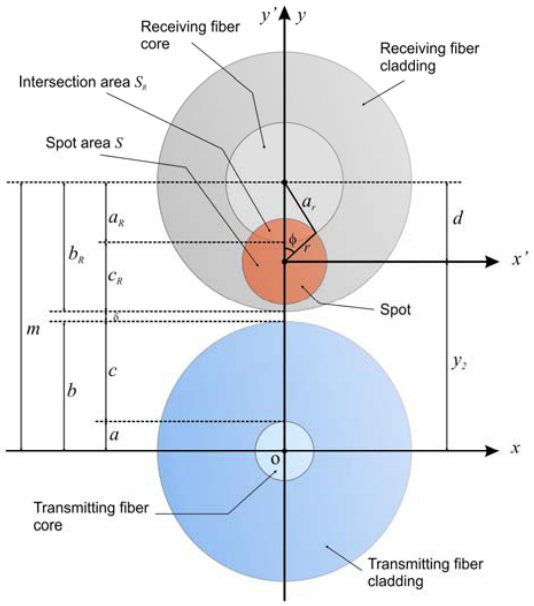


Fig.2 Geometric scheme showing transmitting and receiving fibers and the light spot impinging receiving one.

*2.2.2. Spot position*

Analyzing only the central ray of the reflected beam, knowing its position and angle ($y_1$, $\alpha_1$) at the membrane and using ABCD matrix, it is possible to determine the position and angle ($y_2$, $\alpha_2$) at the receiving fiber. Since $\theta$ is quite small, a paraxial approximation and the following ABCD matrix can be used:

$$\begin{bmatrix} y_2 \\ \alpha_2 \end{bmatrix} = \begin{bmatrix} 1 & d_o \\ 0 & 1 \end{bmatrix} \begin{bmatrix} 1 & 0 \\ -1/f & 1 \end{bmatrix} \begin{bmatrix} 1 & d_1 \\ 0 & 1 \end{bmatrix} \begin{bmatrix} y_1 \\ \alpha_1 \end{bmatrix} \tag{12}$$

As can be seen in Fig. 1, it was stated that $y_1 = 0$ and $\alpha_1 = 2\theta$. With (12) one can vary $d_1$ or $\theta$ parameter to find the spot position $y_2$.

*2.2.3. Integration limits*

In order to determine the integration limits $r_1$ and $r_2$, the spot position was divided in four regions. The first region initiates when the spot starts to enter the core of receiving fiber and it ends immediately after spot enters completely on core, which means

$$a_r - w \le d \le a_r + w$$

and the integration limits are

$$\begin{cases} r_1 = d - a_r \\ r_2 = w \end{cases} \quad (13)$$

The second region occurs when spot is completely on core until the center of spot reach the center of core, i.e.,

$$0 \le d < a_r - w ,$$

and the integration limits are

$$\begin{cases} r_1 = -w \\ r_2 = w \end{cases} \quad (14)$$

The integral is considered symmetric for $d < 0$ and the third and fourth regions are symmetric to first and second, respectively.

## 3. Results

The results presented in this section refer to static calibration curves of microphone. The first curve was obtained varying the tilt angle of membrane, $\theta$, to a fixed position $d_1$. The second curve was obtained varying the position $d_1$ to a fixed angle $\theta$.

### *3.1. Microphone parameters*

The fiber optical microphone mounted in laboratory was built using a light source, two step-index optical fibers, a lens, a reflective membrane mounted over translation and rotation stages, and a photodetector. This system is shown in Fig. 3.

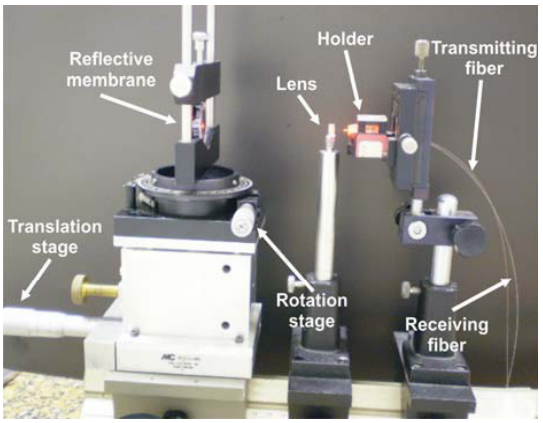


Fig.3 Photography of the fiber optical microphone.

The light source in this case was an He-Ne laser with 633 nm wavelength and 30 mW power. A PIN photodiode OPF480 was employed as photodetector. The reflective membrane used was a dielectric mica film with 19.4 mm radius and 60 μm thickness. The membrane was mounted in a circular support, fixed at the borders. The purpose of this work was not a membrane analysis, and then its parameters were not subject of concern. The transmitting fiber has the following characteristics: monomode, 1330 nm operating wavelength, $a$ = 4 μm, $b$ = 60 μm, and refraction indexes $n_1$ = 1.465 (core) and $n_2$ = 1.460 (cladding), resulting in $NA \cong 0.12$. The receiving fiber has the following relevant characteristics: multimode, $a_R$ = 13 μm, and $b_R$ = 60 μm. The gap between fibers is regarded as $\delta = 0$, then

$m$ = 120 μm. The lens had a focal distance $f$ = 8 mm. As mentioned before $y_1 = 0$, $\alpha_1 = 2\theta$. The calculated parameters are $\theta_o \cong 121$ mrad and $d_o \cong 7.96$ mm. The spot radius was considered as $w$ = 12 μm and $\Lambda = 2$.

Experimental and simulation results are compared in the next sections.

### *3.2. Tilt angle variation*

Firstly, to evaluate the η variation as a function of tilt angle variation θ, for a given constant d1, it was used (12) to determine the y2 position, d position with (10) and the integration limits r1 and r2 with (13) or (14). Then η was calculated using (9). This calculation was done through computer simulation to each $\theta$ value, and the result was normalized. The set of the following parameters were used: $d_1$ = 60 mm, and $\theta$ ranges from 5 to 10 mrad. Fig. 4 displays the simulation result for $\eta$ as function of $\theta$ in the black solid line.

The measurement was done using a rotation stage to vary membrane angle, maintaining distance $d_1$ = 60 mm. The photodetector output was measured to each angle, measured with the rotation stage scale, and the result was normalized. The experimental result is shown in Fig. 4 in the red markers.

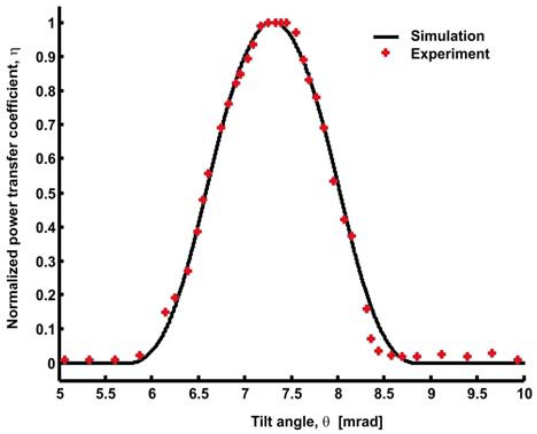


Fig.4 Experimental and simulation curves of power transfer coefficient $\eta$ versus $\theta$ variation.

The curve showed in Fig. 4 indicates that small variations in membrane angle, $\theta$, can cause large variations in $\eta$. For a $\eta$ variation from 10% to 90% it is necessary a tilt angle variation of approximately 0.85 mrad.

Regarding the positive slope of curve and the experimental data, the calibration factor obtained was approximately 98 μrad/V, which means that a 1 V increase at the photodetector output corresponds to a increase of 98 μrad in tilt angle.

### *3.3. Longitudinal displacement*

Secondly, it is evaluated how longitudinal variation in distance between membrane and lens, $d_1$, can cause variations on power transfer coefficient $\eta$. Now the variable in (12) is $d_1$ and to each value of it, one can determine $y_2$, $d$, $r_1$, and $r_2$. The computational simulation was done to a fixed $\theta$, approximately equals to 8.3 mrad. This angle is the one which gives the maximum output to the initial value of $d_1$. In this case, $d_1$ ranges from 60 to 200 mm. The result was normalized and is shown in the black solid line in Fig. 5.

The membrane support was fixed in a translation stage with a micrometer to provide longitudinal displacement, or $d_1$ variation. Then to each position $d_1$ was measured the optical intensity with the photodetector. The measurement was done for $d_1$ from 60 to 83 mm due to translation stage limitation. This curve is shown in red markers in Fig. 5 and it was normalized to compare with simulation.

In Fig. 5 one can realize that a large displacement $d_1$ is necessary to have optical amplitude modulation. Note

that a variation from 10% to 90% needs a displacement of approximately 80 mm. In other words, regarding that membrane movement is a longitudinal displacement, the microphone would have a very low sensitivity.

The calibration factor obtained to this curve was -8.9 mm/V, which means that a 1 V decrease in output voltage corresponds to an increase of approximately 8.9 mm in distance between membrane and lens.

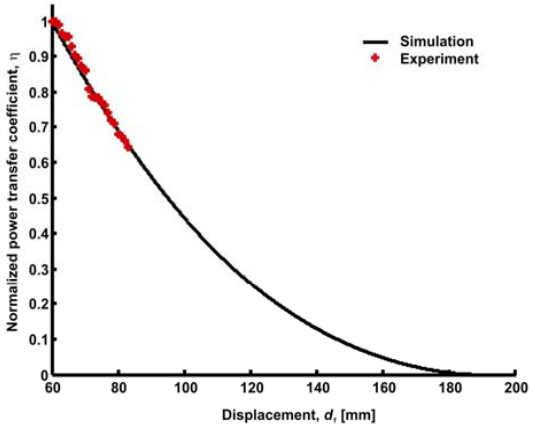


Fig.5 Experimental and simulation curves of power transfer coefficient $\eta$ versus $d_l$ variation.

## 4. Conclusion

According results obtained by computational simulation and corroborated by experiment, to obtain a modulation of light correspondent to an output voltage of 1 V, through longitudinal displacement, it is necessary an unrealistic movement of membrane around 8.9 mm. On the other hand, to obtain the same amount of light modulation, through membrane tilt angle variation, it is necessary only 98 μrad. As can be concluded, the results indicated that the main modulation parameter of this microphone is the membrane tilt angle variation instead the membrane longitudinal displacement. This occurs as a consequence of the collimating and focusing lens effect. It is important to point out that the presented result clarifies the misunderstanding of the two lens microphone [7], in which the authors use the back and forward displacement of membrane to explain the light intensity modulation.

Physically, the tilt angle variation is due to actual membrane movement, which is free on center to displace and it is fixed at the border. This center displacement causes a membrane curvature. Such curvature corresponds to a tilt angle, especially if the light beam provided by transmitting fiber is positioned off center of membrane. Also, since membrane has a small diameter, about 19.4 mm, the actual longitudinal membrane movement is less than 1 mm, which cannot produce a detectable modulation of light.

Analyzing the characteristic curve of power transfer coefficient versus tilt angle one can realize that it presents linear regions appropriated to choose a suitable static operation point, in which membrane tilt angle is converted in optical power variation. To obtain high sensitivity and maximum dynamic range, the static operation point must be achieved setting the angle $\theta$ to drop $\eta$ to half of its maximum value. At this point, the microphone can be used to detect the dynamic vibration of membrane, or the acoustic waves. This use was shown before by the authors in [8].

## Acknowledgements

Work supported by the National Counsel of Technological and Scientific Development, CNPq. The authors wish to thank the Electronic Warfare Laboratory, LABGE, of ITA by some optical components help.

## References

[1] J.P.F. Wooler, B. Hodder and R.I. Crickmore, "Acoustic properties of a fibre-laser microphone", *Meas. Sci. Technol.*, vol. 18, pp.884-888, Feb. 2007.

[2] P. McDowell, B. Bourgeois, P. J. McDowell, S. S. Iyengar, J. Chen, "Relative positioning for team robot navigation", *Autonomous Robots.*, vol. 22, nº.5, pp.133-148, Feb. 2007.

[3] C. M. Traweek, T. A. Wettergren, "Efficient Sensor Characteristic Selection for Cost-Effective Distributed Sensor Networks", *IEEE Journal of Oceanic Engineering,* vol. 31, nº.2, pp.480-486, Apr. 2006.

[4] M. S. NessAiver, M. Stone, V. Parthasarathy, Y. Kahana, A. Paristky "Recording High Quality Speech During Tagged Cine-MRI Studies Using a Fiber Optic Microphone", *Journal of Magnetic Resonance Imaging 23:92-97*, 2006.

[5] J.A. Bucaro, N. Lagakos, "Lightweight fiber optic microphones and accelerometers", *Rev. Sci. Instrum.*, vol. 72, nº 6, pp.2816-2821, Jun. 2001.

[6] J. A. Bucaro, N. Lagakos, B. H. Houston, "Miniature, high performance, low-cost fiber optic microphone", *J. Acoust. Soc. Am.*, vol. 118, pp.1406-1413, Sep. 2005.

[7] M. Feldmann and S. Büttgenbach, "Microoptical Distance Sensor with Integrated Microoptics applied to an Optical Microphone", *IEEE Sensors 2005*, Irvine, CA, USA, pp.769-771, Nov. 2005.

[8] J. M. S. Sakamoto, E. C. Pimenta Jr., G. M. Pacheco, "Analysis of a single lens fiber optical microphone configuration", MOMAG 2008, pp. 391-395, 2008.